

## RESEARCH ARTICLE

# Heterogeneity of neuromasts in a fish without lateral line canals: the pufferfish (*Takifugu obscurus*) model

Chao Li<sup>1,2,3</sup>, Xiaojie Wang<sup>1,2,3</sup>, Jianyong Wu<sup>4</sup>, Xuguang Zhang<sup>1,2,3</sup>, Chunxin Fan<sup>1,2,3</sup>, Hongyi Guo<sup>1,2,3</sup> and Jiakun Song<sup>1,2,3,\*</sup>

## ABSTRACT

Fish detect water motion with their mechanosensory lateral line. The basic functional unit of the lateral line is the neuromast. In most fish species, neuromasts are located in lateral line canals (canal neuromasts) or on the skin (superficial neuromasts). In this paper, we describe the lateral line system of the pufferfish, *Takifugu obscurus*. If threatened, this fish inflates its body by sucking water into the esophagus. Pufferfish lack a canal system but have neuromasts located directly on the skin or in open grooves. Each groove houses tall, medium and short neuromasts, based on the height of their pedestal. One or more medium neuromasts were always located between two tall neuromasts, and the short neuromasts were scattered between them. Tall neuromasts showed phasic responses to water jets, similar to the canal neuromasts of other fish species. In contrast, the medium and short neuromasts showed tonic responses to water jets. The response properties of nerve fibers that innervated the medium and short neuromasts were similar to those of the superficial neuromasts found in other fish species. Our results suggest that each groove of a pufferfish has two functional groups of neuromasts. This may allow pufferfish to extract spatial and temporal hydrodynamic information, despite the changes in body shape that occur during and after inflation. The short neuromasts at the bottom of a groove most likely supplement the medium neuromasts when the body is maximally inflated.

**KEY WORDS:** Lateral line groove, Tall neuromast, Medium neuromast, Short neuromast, Neuromast pedestal

## INTRODUCTION

Water movements are an important source of information for aquatic animals. Fish and some aquatic amphibians can detect water movements with their lateral line (Dijkgraaf, 1963; Bleckmann, 1994). The basic functional unit of the lateral line is the neuromast (NM). Two types of lateral line NMs can be distinguished: superficial neuromasts (SNs), which are freestanding on the skin, and canal neuromasts (CNs), which are located in lateral line canals. Lateral line NMs consist of discrete clusters of sensory hair cells, supporting cells and mantle cells (Münz, 1985). At their apical surface, the sensory hair cells carry a ciliary bundle.

Each bundle consists of several stereovilli of graded length and a single kinocilium. Both stereovilli and kinocilium project into a gelatinous cupula (Mohr and Görner, 1996).

CNs are larger than SNs and contain more hair cells (Song and Northcutt, 1991a). An afferent nerve fiber that innervates a CN never branches, i.e. it never innervates more than one CN (Münz, 1985; Bleckmann and Zelick, 2009). Afferent nerve fibers that innervate SNs usually innervate more than one SN (e.g. Münz, 1985; Song and Northcutt, 1991a,b). If so, these NMs form a functional unit (Münz, 1979, 1985). Lateral line NMs are highly sensitive to water motion: SNs respond in proportion to water velocity; CNs respond in proportion to water acceleration (Kroese and Schellart, 1992).

Hydrodynamic stimuli produced by behaving or freely swimming animals have a 3D extension and vary with respect to duration and frequency–amplitude content (Bleckmann, 1994). Therefore, the spatial as well as the temporal patterns of a hydrodynamic stimulus contain important information. Behavioral studies have shown that SNs and CNs serve different behaviors (Montgomery et al., 1997; Mekdara et al., 2018). SNs are involved in the detection and encoding of large-scale stimuli (Montgomery et al., 1997; Coombs, 2001), i.e. in the integration of spatial information (Coombs, 2001). In contrast, CNs provide spatial details of a hydrodynamic stimulus that allows fish to orient towards the stimulus source and/or to respond to rapidly changing water motions.

Until recently, fast swimmers or fish that live in running water were believed to have a large number of lateral line canals and/or branched canals and few SNs. In contrast, slow swimmers or species that live in slow-flowing waters were believed to possess reduced canals and an increased number of SNs (Dijkgraaf, 1963; Mogdans et al., 2003). However, in a more recent study, this could not be confirmed (Beckmann et al., 2010). Some fish species lack lateral line canals. In these fish, the CNs identified on the basis of morphological and developmental studies have been described as either SNs or ‘replacement neuromasts’ (Webb, 1989). For example, all Tetraodontiformes lack lateral line canals (e.g. pufferfishes, triggerfishes, ocean sunfishes) (Nakae and Sasaki, 2005, 2010; Holcroft and Wiley, 2008; Song et al., 2010); consequently, in these fish, all NMs are located on the skin or in grooves.


In pufferfish, lateral line canals are reduced to grooves. Pufferfish show a unique avoidance behavior: if threatened, they inflate their body by sucking water into the esophagus (Zhao et al., 2010; Wang et al., 2015). This study describes the physiology and morphology of the pufferfish lateral line. In addition, we studied the response properties of pufferfish NMs. Our results suggest that pufferfish have a unique lateral line system that functions not only before but also during and after body inflation.

## MATERIALS AND METHODS

Newly hatched and adult pufferfish, *Takifugu obscurus* (Abe 1949) were used for the experiments. Fish were obtained from the fish

<sup>1</sup>Institute for Marine Biosystem and Neuroscience, Shanghai Ocean University, Shanghai 201306, China. <sup>2</sup>National Demonstration Center for Experimental Fisheries Science Education (Shanghai Ocean University), Shanghai 201306, China. <sup>3</sup>International Research Center for Marine Biosciences at Shanghai Ocean University, Ministry of Science and Technology, Shanghai 201306, China. <sup>4</sup>Department of Neuroscience, Georgetown University, Washington, DC 20007, USA.

\*Author for correspondence (Songj@si.edu)

 J.S., 0000-0002-6436-4773

hatchery of Shanghai Fisheries Research Institute, housed in aerated, filtered freshwater aquaria at  $26\pm 2^\circ\text{C}$  and fed with commercial fish twice a day. Prior to surgery, pufferfish were anesthetized by immersion in 0.03% tricaine methanesulfonate (MS-222, Sigma, Poole, UK). All animal protocols were approved by the Review Committee for the Use of Animal Subjects of Shanghai Ocean University.

### Morphology and distribution

The morphology and distribution of NMs was examined by Daspei (in larval fish) or Methylene Blue staining. For Daspei staining, the fish were immersed for 30 min in water that contained  $0.04\text{ mg ml}^{-1}$  Daspei {2-[4-(dimethylamino)styryl]-*N*-ethylpyridinium iodide; MW380.27, Life Technologies, Molecular Probes, Eugene, OR, USA}. Methylene Blue staining was achieved by placing the fish in a 0.005% Methylene Blue solution until even the smallest NMs were stained.

The morphology of NMs was examined in histological sections. Five specimens (standard body length, SL: 12 cm) were fixed by AFA (90 ml 80% ethanol, 5 ml formaldehyde, 5 ml glacial acetic acid), and epithelial tissue and proximal portions of the lateral line groove ( $5\text{ mm}\times 5\text{ mm}\times 2\text{ mm}$ ) were processed for paraffin embedding. Cross-sections and sagittal sections along the groove were prepared and stained with hematoxylin/eosin (HE) and observed under an Axio Observer Z1 microscope (Carl Zeiss, Oberkochen, Germany).

In 20 fish, lateral line NMs were also examined by scanning electron microscopy (SEM). Fish were killed by an overdose (0.3%) of MS-222 and fixed in 4% paraformaldehyde in  $0.1\text{ mol l}^{-1}$  phosphate-buffered saline (pH 7.4) for several days, and then post-fixed in 2.5% glutaraldehyde in  $0.1\text{ mol l}^{-1}$  phosphate-buffered saline (pH 7.4) for 12 h (or overnight). Evaluation was done with a Hitachi SEM S-3400 NII (Tokyo, Japan). Polarization of hair cells was determined from the SEM images. The surface of the NMs was cleaned with an ultrasonic bath (60 Hz for 30–60 s on fixed samples) to ablate the stereovilli and kinocilium. The height of

the NMs (distance from the base to the sensory epithelium of the NM) was measured from the SEM images using Image J software. In order to capture all NMs of a groove, grooves were hemisected along the long axis.

### Lateral line nerves

The peripheral extension of the lateral line nerves was examined by gross dissection with the aid of Sudan Black staining solution (Song and Northcutt, 1991a) and by DiI tracing (12 specimens, 11.4–15 cm SL). DiI crystals (1,1'-dioctadecyl-3,3,3',3'-tetramethylindocarbocyanine perchlorate, C7000, Molecular Probes) were dissolved in dimethylformamide (2.5%). Tall NMs and medium NMs were injected with DiI on the supraorbital line and trunk line in order to visualize the innervation patterns of a single NM. After a week, fish were killed with an overdose of MS-222 and fixed in 4% paraformaldehyde, then stored in the dark ( $4^\circ\text{C}$ ). Samples were dissected and observed with a fluorescence stereomicroscope (Discovery.V12, Carl Zeiss).

### Electrophysiology

The responses of NMs to water movements were examined in skin preparations. Animals ( $17.12\pm 0.71\text{ cm SL}$ ) were anesthetized on ice. Thereafter, a piece of skin on the trunk lateral line (TRL), containing several NMs and the lateral line nerve, was separated from the fish and immersed in Ringer's solution ( $91\text{ mmol l}^{-1}\text{ NaCl}$ ,  $2.1\text{ mmol l}^{-1}\text{ KCl}$ ,  $1.8\text{ mmol l}^{-1}\text{ MgCl}_2\cdot 6\text{H}_2\text{O}$ ,  $20\text{ mmol l}^{-1}\text{ NaHCO}_3$ ,  $4\text{ mmol l}^{-1}\text{ glucose}$ ,  $2.6\text{ mmol l}^{-1}\text{ CaCl}_2$ ). For recordings, skin preparations were pinned on silicone rubber with the NMs facing upward. To record spikes from different NMs, we separated individual afferents from the lateral line nerve bundle. For recording, the free ending of the nerve innervating the NMs was sucked into a fire-polished glass pipette (suction electrode).

The tip diameter of the suction electrode was made slightly smaller than the nerve from which recordings were obtained; usually, for a nerve ending with a diameter of  $\sim 100\text{ }\mu\text{m}$ , a suction

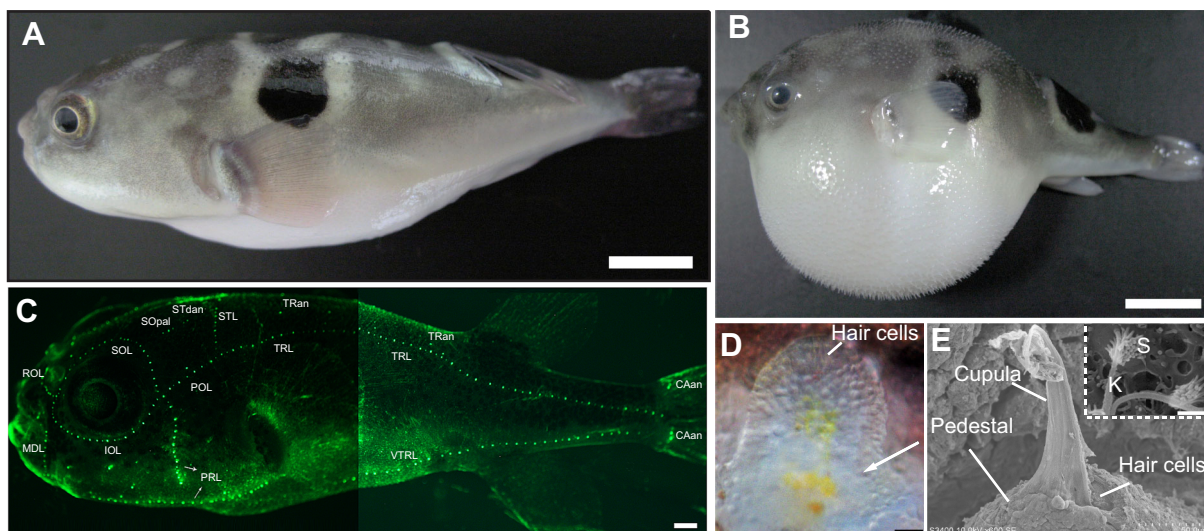


**Fig. 1. The morphology of pufferfish (*Takifugu obscurus*) and the distribution of neuromasts (NMs).** (A) Lateral view of an uninflated pufferfish. Scale bar: 1 mm. (B) Lateral view of an inflated pufferfish. Scale bar: 1 mm. (C) Lateral view of a pufferfish stained with Daspei, illustrating the relative positions and extent of cephalic and trunk lateral lines as well as accessory lines. CAan, caudal accessory neuromasts; IOL, infraorbital line; MDL, mandibular line; POL, postotic line; PRL, preopercular line; ROL, rostral line; SOL, supraorbital line; SOpal, posterodorsal supraorbital accessory neuromasts; STdan, dorsal supratemporal accessory neuromasts; STL, supratemporal line; TRan, trunk accessory neuromasts; TRL, trunk lateral line; VTRL, ventral truck line. Scale bar: 500  $\mu\text{m}$ . (D) A neuromast on a pedestal (indicated by the white arrow); the cilia of the hair cells are visible under DIC microscopy. Scale bar: 50  $\mu\text{m}$ . (E) A ciliary bundle formed by the hair cells protrudes into the cupula. Inset: a pair of hair cells with opposite polarity (K, kinocilium; S, stereovilli). Scale bar: 1  $\mu\text{m}$ .



electrode with a tip diameter of  $\sim 80 \mu\text{m}$  was used. This ensured a good signal-to-noise ratio. Recordings were done with a custom-made amplifier ( $1000\times$  gain, bandwidth 0.05–3000 Hz). Data were sampled with Spike 2 (version 8.04, Cambridge Electronic Design, Cambridge, UK).

Water-jet stimuli were applied using pressure and a glass pipette. The diameter of the tip opening of the glass pipette was about  $70 \mu\text{m}$ . The pressure used to generate a water jet was adjusted according to the sensitivity of the respective NM. Both pressure and duration of the water jet were controlled by a digital micro-injector system (Tritech Research, Inc., Los Angeles, CA, USA). After identifying the NM (or NMs) that was (were) innervated by the nerve fiber from which recordings were made, a micromanipulator was used to position the stimulating pipette such that the applied water jet was parallel to the groove that housed the NMs.

## RESULTS

### Morphology of the NMs

The lateral line system of *T. obscurus* consists of mechanoreceptive NMs located in seven pairs of cephalic grooves, two pairs of trunk grooves and eight pairs of accessory NM lines (Fig. 1). Some NMs were positioned on a ‘stalk’ or ‘pedestal’ (Fig. 1D,E). The staircase-like arrangement of the stereovilli and the position of the kinocilium determine the direction in which a hair cell is most sensitive (Song and Northcutt, 1991a) (Fig. 1E). Many of the NMs were

located in a groove and were positioned on a pedestal. Various pedestal heights were observed (Fig. 2A). Three types of NMs could be distinguished: tall, medium and short. Tall NMs had the tallest pedestal ( $124.93 \pm 1.26 \mu\text{m}$ , mean  $\pm$  s.e.m.,  $n=15$ ; white arrowheads in Fig. 2A), the largest diameter and the greatest number of hair cells (Fig. 2B,F). Medium NMs (white arrows in Fig. 2A), had a shorter pedestal and fewer hair cells than the tall NMs (Fig. 2C,G). Short NMs had the shortest pedestal or sat directly on the bottom of a groove (asterisks in Fig. 2A). They also had the fewest number of hair cells (Fig. 2D,H). Medium NMs were always located in between two tall NMs, and the short NMs were scattered between them. As a result, the tall NMs, medium NMs and short NMs formed a particular arrangement in each lateral line groove (Fig. 2A,E).

We also investigated the orientation of the NMs. With respect to their most sensitive axis, the orientation of tall NMs was parallel to the long axis of the groove (Fig. 2I,J). In contrast the medium and short NMs were oriented perpendicular to the long axis of the groove (Fig. 2K,L).

To understand the growth of medium and short NMs, we counted the number of NMs in 12 fish that differed in size (2.75–19.57 cm SL). The results indicate that NM number is positively correlated with body size. The number of short NMs increased at a much higher rate than the number of tall and medium NMs (Fig. 3A), while the number of tall and medium NMs increased at about the same rate.

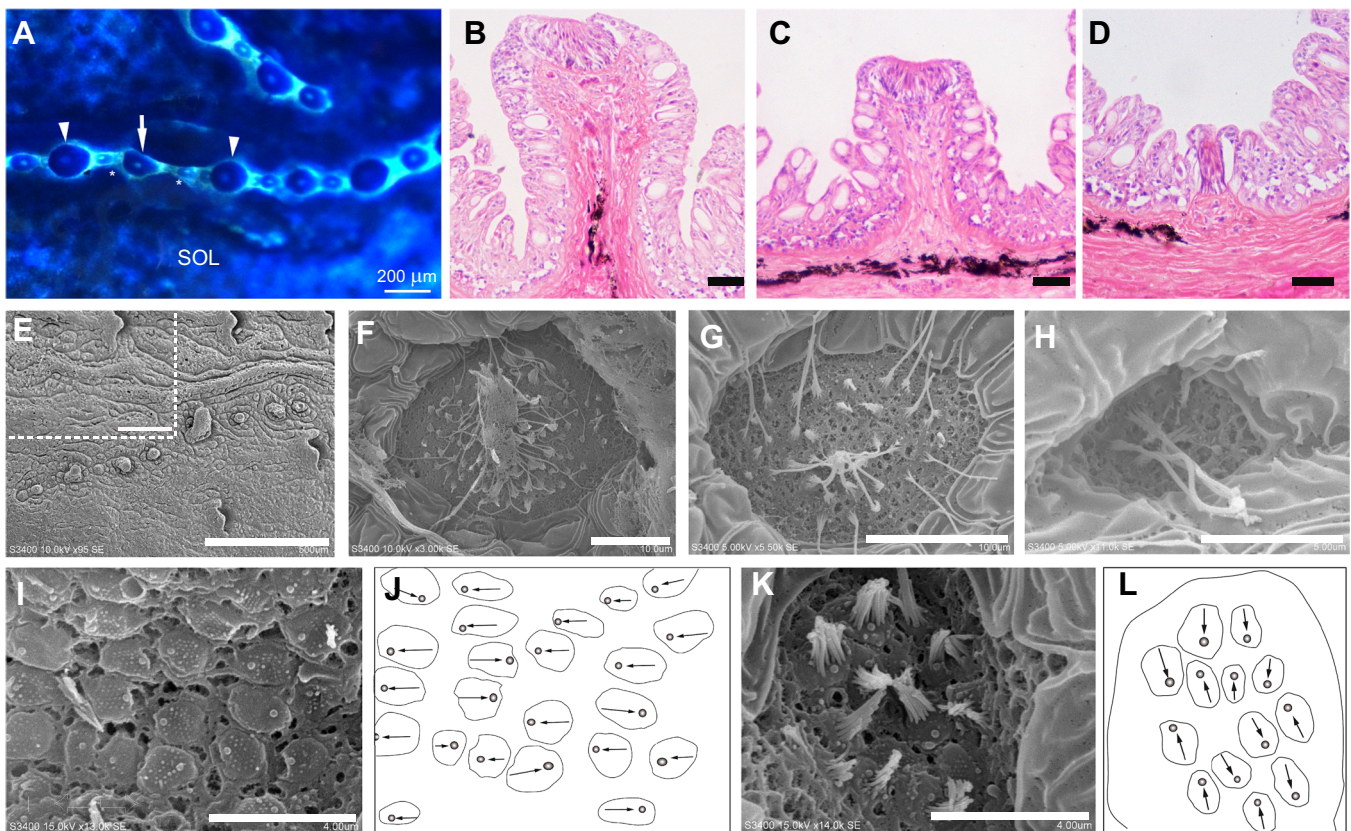


**Fig. 2.** The arrangement of NMs in the lateral line groove of a pufferfish. (A) Three types of NMs form a consistent pattern: a medium NM (arrow) sits between two tall NMs (arrowheads). Short NMs (asterisks) are always scattered among them. Scale bar:  $200 \mu\text{m}$ . (B–D) Cross-sections stained with hematoxylin/eosin (HE) reveal the morphologies of the three types of NMs. Scale bars:  $25 \mu\text{m}$ . (E–H) The microstructure of three types of NMs can be studied with scanning electron microscopy (SEM). Scale bars:  $500 \mu\text{m}$  (E),  $200 \mu\text{m}$  (E, inset),  $10 \mu\text{m}$  (F,G) and  $5 \mu\text{m}$  (H). E shows three types of NMs forming a consistent pattern; B and F show a tall NM; C and G are medium NMs; D and H are short NMs. (I–L) Orientation of the tall and medium NMs along the trunk line of *T. obscurus* (13.5 cm standard body length). (I,J) The most sensitive axis (indicated by arrows) of the tall NMs is along the long axis of the groove (R, rostral; C, caudal); (K,L) the medium NMs are oriented vertically (arrows) with respect to the long axis of the groove. Scale bar in I and K:  $4 \mu\text{m}$ .

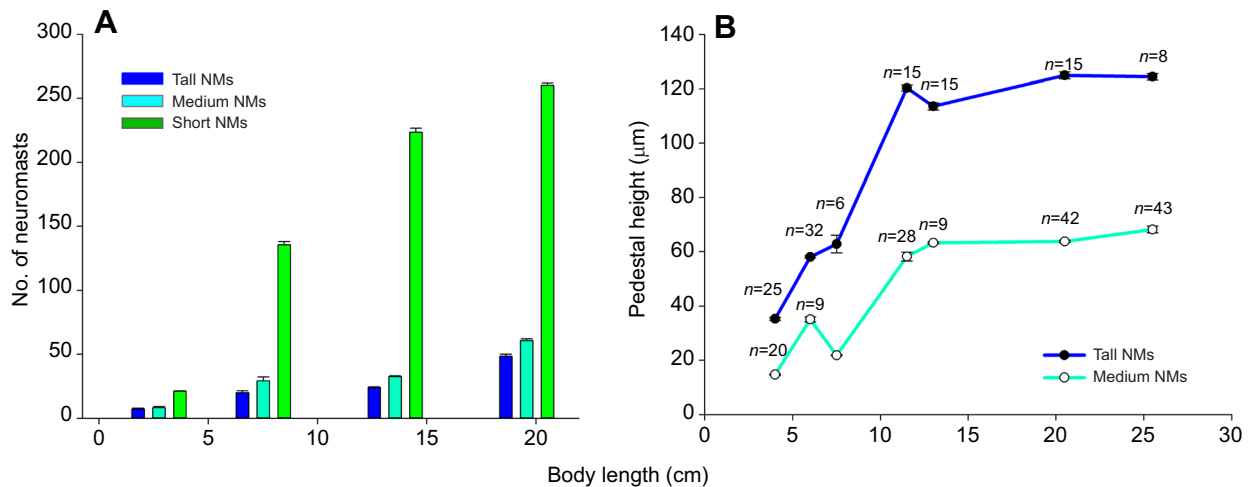


**Fig. 3. Neuromast growth.** Number of NMs on the trunk line of *T. obscurus* (A) and height of pedestals (B) as function of fish size.

Next, we measured the length of the pedestal of NMs during fish growth using a range of fish sizes (4.0–25.5 cm SL). During growth, the height of the pedestals kept increasing for the tall and medium NMs until fish reached a body length (SL) of about 11.5 cm. At this point, the height of the pedestals of the tall and medium NMs remained constant, but the pedestals of the tall NMs ( $n=11$ ) were almost twice as high as the pedestals of the medium NMs ( $n=9$ ) (Fig. 3B). These length differences indicate that medium NMs do not transform into tall NMs during fish growth.

#### Innervation pattern of the NMs

The innervation pattern of the tall and medium NMs was different (Fig. 4). An afferent nerve fiber that innervated a medium NM always had several collaterals that innervated adjacent short NMs (Fig. 4C). Each tall NM was innervated by afferent nerve fibers that never branched to nearby NMs (Fig. 4C). This innervation pattern indicates that the medium NMs and their neighboring short NMs form a functional unit. In contrast, each tall NM represented a single unit.

#### Electrophysiological properties of the NMs

The trunk lateral line nerve (Fig. 5A,B) was chosen for the electrophysiological investigations. Spikes varied in amplitude, response frequency and spontaneous activity, suggesting that different NMs were innervated by nerve fibers that differed in diameter. In particular, the tall, medium and short NMs could be distinguished by the amplitude of their evoked spikes.

The orientation of tall NMs was parallel to the long axis of the groove, and the tall NMs responded with more spikes to the jet orientation parallel to the groove than to the jet orientation perpendicular to the groove (data not shown). The stimulating pipette as well as its applied water jet was along the groove, either parallel or perpendicular during the stimulation.

Tall NMs had a high spike amplitude ( $153.38 \pm 9.47 \mu\text{V}$ , mean  $\pm$  s.d.,  $n=1173$ ) (Fig. 5C,D), suggesting that they were innervated by thick axons (green arrows in Fig. 5B). In comparison, medium/short NMs had a low spike amplitude ( $68.48 \pm 6.19 \mu\text{V}$ , mean  $\pm$  s.d.,  $n=1389$ ) (Fig. 5E,F), suggesting that they may be innervated by thin axons (e.g. blue arrows in Fig. 5B).

Because spike amplitude varied with recording conditions (better seals resulted in higher spike amplitudes), we needed a

standard to define high- and low-amplitude spikes in each recording. We used the amplitude of spontaneous spikes as a relative scale for comparing spike amplitudes. For each recording, more than 1000 spontaneous spikes were collected. The mean amplitude of all spontaneous spikes was defined as 100% (Fig. 5G). High-amplitude spikes ( $n=1173$ ) were evoked by stimulating the tall NMs; the amplitude of these spikes was about 275% of the amplitude of the spontaneous spikes (Fig. 5G). Low-amplitude spikes ( $n=1389$ ) were recorded from medium and short NMs; the amplitude of these spikes was similar to the amplitude of the spontaneous spikes (Fig. 5G).

The responses of the high- and low-amplitude spikes to a water jet stimulus were different. The high-amplitude spikes demonstrated a phasic response, i.e. a transient burst occurred at the onset of a water jet stimulus (Fig. 5C,D), suggesting that the tall NMs sense transient water movements. In contrast, low-amplitude spikes showed a tonic response, i.e. a stable discharge rate during the entire duration of the stimulus (Fig. 5E,F). This suggests that the medium and short NMs are sensitive to constant water flow. To further distinguish phasic from tonic responses, we divided each response (10 psi/1 s) into 10 equal time periods and counted the number of spikes for each period (Fig. 5H). The tall NMs showed a typical phasic firing pattern (green bars) with the number of spikes decreasing while a persistent water jet was applied with constant pressure. In contrast, the medium/short NMs showed tonic responses (blue bars), and the number of spikes remained relatively constant throughout stimulation (Fig. 5H).

A model which shows how the two groups of NMs could function is given in Fig. 6. Medium NMs are always located between two tall NMs, and the short NMs are distributed between the medium and tall NMs (Fig. 6). The physiological data indicate that the tall NMs show phasic responses to the hydrodynamic stimulus, while the medium/short NMs show a tonic response to the stimulus.

This suggests that the three types of NMs belong to two functional groups of NMs that encode different aspects of the hydrodynamic stimulus. Tall NMs encode acceleration like the CNs of other fish species, and the medium and short NMs respond like the SNs of other fish species, i.e. they are sensitive to water velocity.

#### DISCUSSION

One of the most intriguing characteristics of the pufferfish is its extensible body, which can inflate to a balloon-like shape (Fig. 1B) after the fish has swallowed water into a flexible but tough



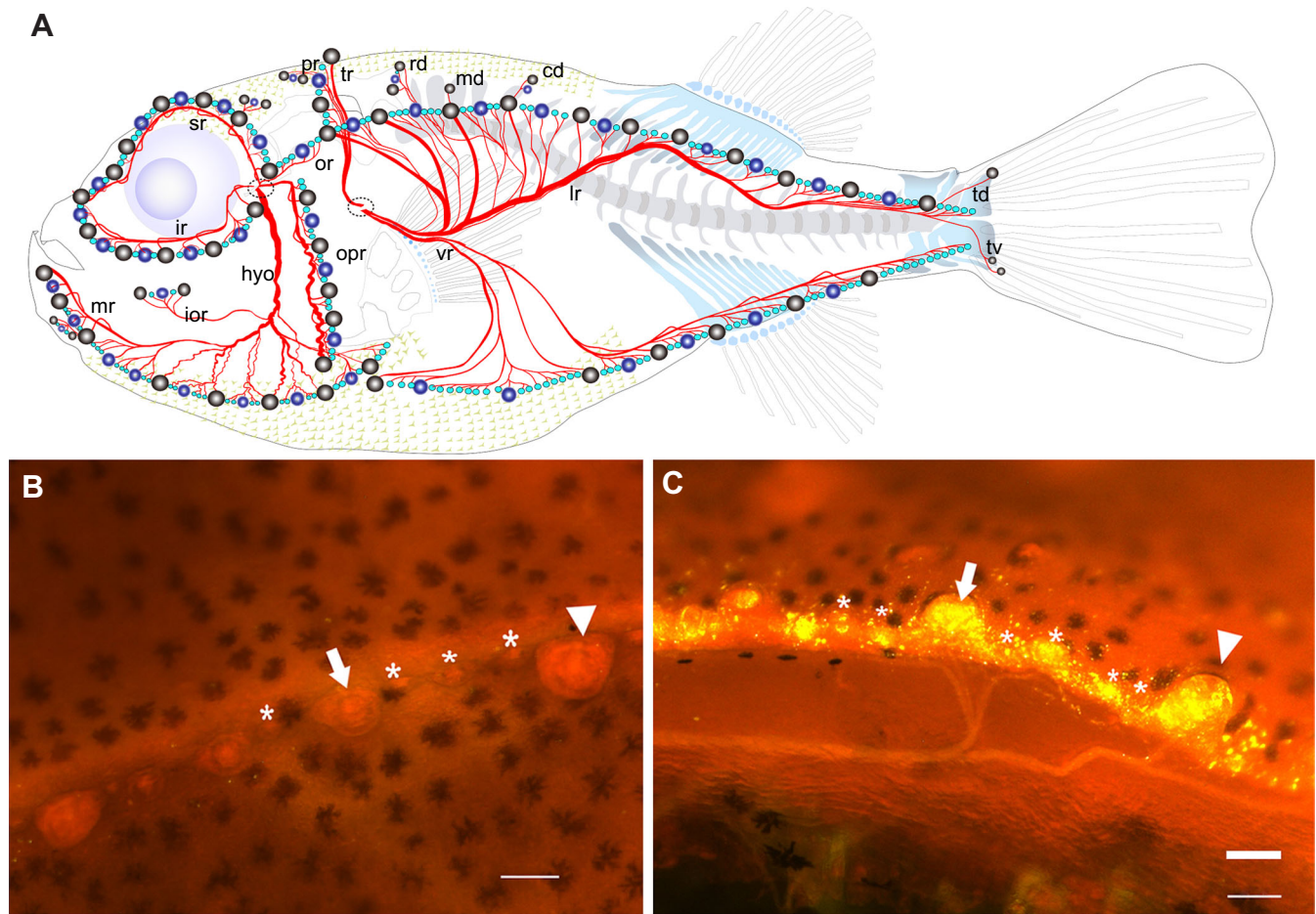


**Fig. 4. Innervation pattern of the NMs of *T. obscurus*.** (A) Drawing of the lateral line nerves. The rami of the various lateral line nerves are shown in red. Gray circles: tall NMs; dark blue circles: medium NMs; light blue circles: short NMs. cd: caudal ramule of the dorsal ramus of the PLLN; hyo: hyoid ramus of the ALLNv; ior: infraorbital ramule of the hyoid ramus of the ALLNv; ir: infraorbital ramus of the ALLNv; lr: lateral ramus of the PLLN; md: medial ramule of the PLLN; mr: mandibular ramus of the ALLNv; opr: preoperculo-mandibular ramus; or: otic ramus of the ALLNv; pr: posterior ramule of the temporal ramus of the PLLN; rd: rostral ramule of the PLLN; sr: superficial ophthalmic ramus of the ALLNv; td: dorsal ramule of terminal lateral ramus of the PLLN; tr: temporal ramus of the PLLN; tv: ventral ramule of terminal lateral ramus of the PLLN; vr: ventral ramus of the PLLN; ALLNd: anterodorsal lateral line nerve; ALLNv: anteroventral lateral line nerve; PLLN: posterior lateral line nerve. (B) Top view: Dil was injected into a tall NM (arrowhead) and a medium NM (arrow). Short NMs are indicated by asterisks. (C) An afferent nerve contacts a medium NM and six short NMs (asterisks), while a single tall NM (arrowhead) is innervated by a single afferent nerve in the SOL. Scale bars: 100  $\mu$ m.

esophagus sac (Zhao et al., 2010; Wang et al., 2015). In this study, we examined the lateral line system of pufferfish. This fish shows a unique NM pattern: (1) three types of NM (tall, medium and short) are located on the skin surface in grooves; (2) the three morphological types of NM form a spatial pattern that is retained during fish growth; and (3) there are two functional groups of NMs that can be identified physiologically.

There are several types of lateral line canal in various fish species, including reduced canal systems. In herring *Clupea harengus* (Clupeiformes), the trunk lateral line canal is absent. In the flatfish *Solea solea* (Pleuronectiformes), the infraorbital canals are reduced in adult fish. In the deep-sea fish *Anoplogaster cornuta* (Beryciformes), the canals are reduced to shallow chambers (Blaxter, 1987) and *Phrynichthys wedli* (Lophiiformes) even lacks canal organs (Marshall, 1996). In the black goby, *Gobius niger* (Perciformes), only part of the preoperculo-mandibular canal is found (Marshall, 1986). Differences in lateral line canal morphology occur in many orders of Neopterygii fish, including Tetraodontiformes, the order to which pufferfish belong. The Tetraodontiformes lack lateral line canals; in these fish, all NMs are located in lateral line grooves (Nakae

and Sasaki, 2010; Song et al., 2010). This suggests that diverse lateral line canal/groove patterns reflect important functional differences.

In this study, we found that the three types of pufferfish NMs form two functional groups. The tall, medium and short NMs are located on the tip of pedestals that differ in height. Finger-like pedestals have also been described in the black goby (Marshall, 1986) and in the deep-sea fish *P. wedli* (Marshall, 1996). However, the spatial NM pattern within the grooves of pufferfish has never been reported in other fish species. Our histological and SEM examinations revealed that the tall NMs are larger and possess many more hair cells than the medium NMs. Large and small cupula are affected differently by inertial forces and viscous forces, respectively (Mogdans et al., 2003). A smaller diameter cupula is likely to function as a velocity receptor, whereas a larger diameter cupula mainly functions as an acceleration detector (Mogdans et al., 2003).

We also found differences in hair cell orientation: in the sensory epithelium of the tall NMs, hair cells were oriented with respect to their most sensitive axis, in the direction of the groove. In the medium and short NMs, the orientation of hair cells was perpendicular to the

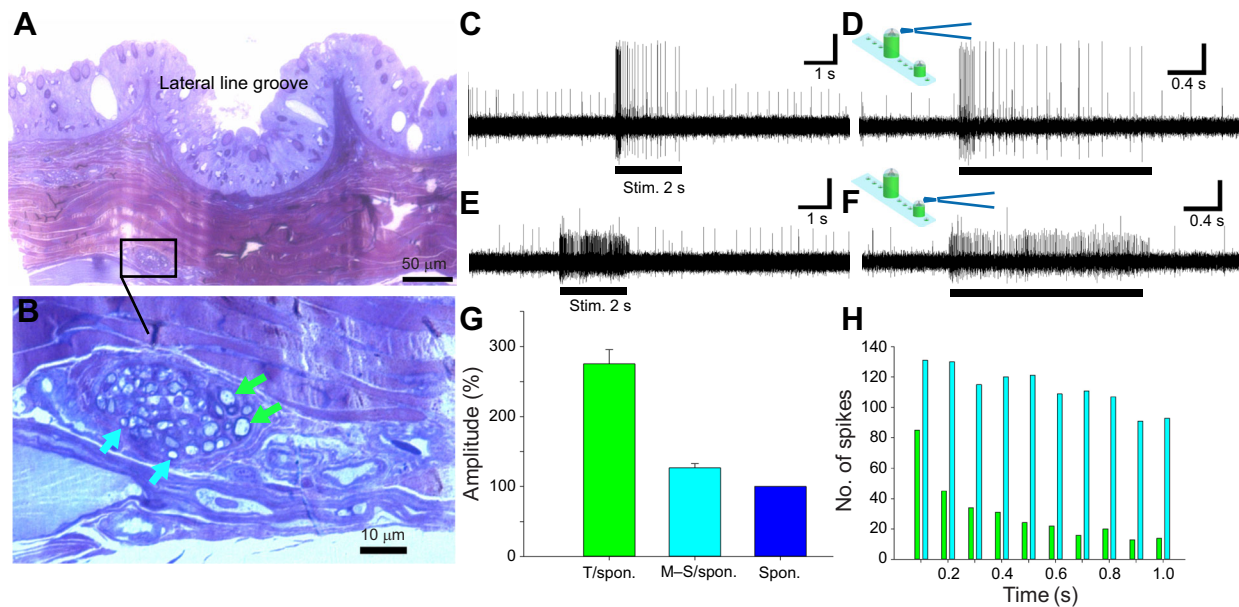


**Fig. 5. Electrophysiology from a lateral line nerve.** (A) Horizontal section of the skin around the trunk lateral line groove. The boxed area, enlarged in B, marks the cross-section of a nerve innervating the lateral line. (B) Axons with large and small diameters are indicated by green and blue arrows, respectively. (C–F) Spikes recorded from the same nerve (diameter: 100  $\mu$ m); the timing of stimulus application is indicated by the thick horizontal lines. The recording was made with a suction electrode (tip diameter: 80  $\mu$ m). The water jet was created by a glass pipette (tip opening: 33  $\mu$ m), and a water jet was generated near the tip. (C,D) When the water jet (5 psi/2 s) was aimed at a tall NM, high-amplitude spikes were evoked; (E,F) when the water jet (10 psi/2 s) was lowered into the groove, low-amplitude spikes were evoked. Traces in C–F have the same vertical scale (60  $\mu$ V). (G) In order to quantify the amplitude of the spikes, the amplitude of the evoked spikes was compared with the amplitude of the spontaneous spikes. The high-amplitude spikes from tall NMs ( $n=1173$ ) were about 275% of the amplitude of the spontaneous spikes (T/spon.= $275\pm 20.39\%$ , mean $\pm$ s.d.). In contrast, the evoked low-amplitude spikes from the medium and short NMs ( $n=1389$ ) were indistinguishable from the amplitude of the spontaneous spikes (M–S/spon.= $126\pm 6.14\%$ , mean $\pm$ s.d.). (H) Firing pattern of the tall and medium–short NMs when stimulated with a water jet. We divided the spiking response (to the 10 psi/1 s stimulus) into 10 equal time periods (for 12 preparations) and plotted the number of spikes occurring in each period. The responses of the tall NM (green bars) were phasic (the number of spikes decreased during jet stimulation). In contrast, the medium/small NMs (blue bars) showed tonic responses (the number of spikes during persistent stimulation only slightly decreased).

long axis of the groove. Therefore, the orientation of the hair cells of the tall NMs matches the orientation of the hair cells in the CNs of other fish species. For example, in the posterior lateral line system of zebrafish, the orientation of the hair cells of primary NMs (which most likely derived from CNs) is parallel to the rostral-caudal axis of the fish, and the orientation of the hair cells of secondary NMs is perpendicular to the rostral-caudal axis of the fish (Ghysen and Dambly-Chaudière, 2007; Ghysen et al., 2014). The functional significance of the various hair cell orientation patterns most likely facilitates the analysis of hydrodynamic information. The convergence of the information of tall and medium NMs could, for instance, provide fish with better directional information. The tall and medium NMs are orthogonally polarized, and the medium NMs and short NMs act as a functional group. Further experiments are needed to fully assess the differences in the response properties of the two neuromast functional groups found in pufferfish.

NMs were counted on fish that differed in size. The relative number of short NMs increased greatly as the fish grew, while the number of tall and medium NMs increased only slowly during development. Their relative numbers stayed the same. The observed growth pattern indicates that the spatial arrangement of the various types of NMs remains throughout the life of a pufferfish, and that short NMs do not transform into other NM types.

To better understand the differences between NM growth patterns, we traced the fate of the medium NMs during fish growth. The results revealed that the length of the pedestal of the two functional types of NMs does not further increase after fish have reached a body length (SL) of about 11.5 cm. This suggests that the different types of NMs

are not transitional phases but are consistent and retained throughout fish growth. Based on the above observation, the tall, medium and short NMs can be considered as distinct, possibly unique types of NMs. Most importantly, two functional groups of NMs exist in the open grooves of the lateral line system of pufferfish.

Another important consideration is that pufferfish have a non-inflated phase and an inflated phase; thus, the two functional groups of NMs most likely provide complementary information for each phase. When not inflated, the pedestal should bring the large NMs out of the boundary layer. This makes these NMs more sensitive to low-frequency stimuli (low-frequency water movements have a thicker boundary layer than high-frequency water movements). When not inflated, the medium/short NMs will receive little, if any, stimulation in the mucus. When inflated, the grooves widen, exposing the short NMs to the flow. In this way, the short NMs function like the ordinary SNs found in other fish species. Therefore, two functional groups of neuromasts are needed for pufferfish to detect hydrodynamic information in the functional and developmental sense.

Another important consideration is the innervation pattern of the NMs. Individual afferents innervating the medium NMs always innervate several neighboring short NMs, while the afferent nerve fibers innervating the tall NMs never branch. The innervation pattern of the medium and short NMs resembles the innervation pattern and the development of the terminal neuromasts of zebrafish and medaka (Wada et al., 2008). This suggests that the two functional groups of pufferfish NMs (tall versus medium/short NMs) originate from different primordia. A single afferent fiber has a lower input resistance if it innervates several NMs; it is less sensitive and has a



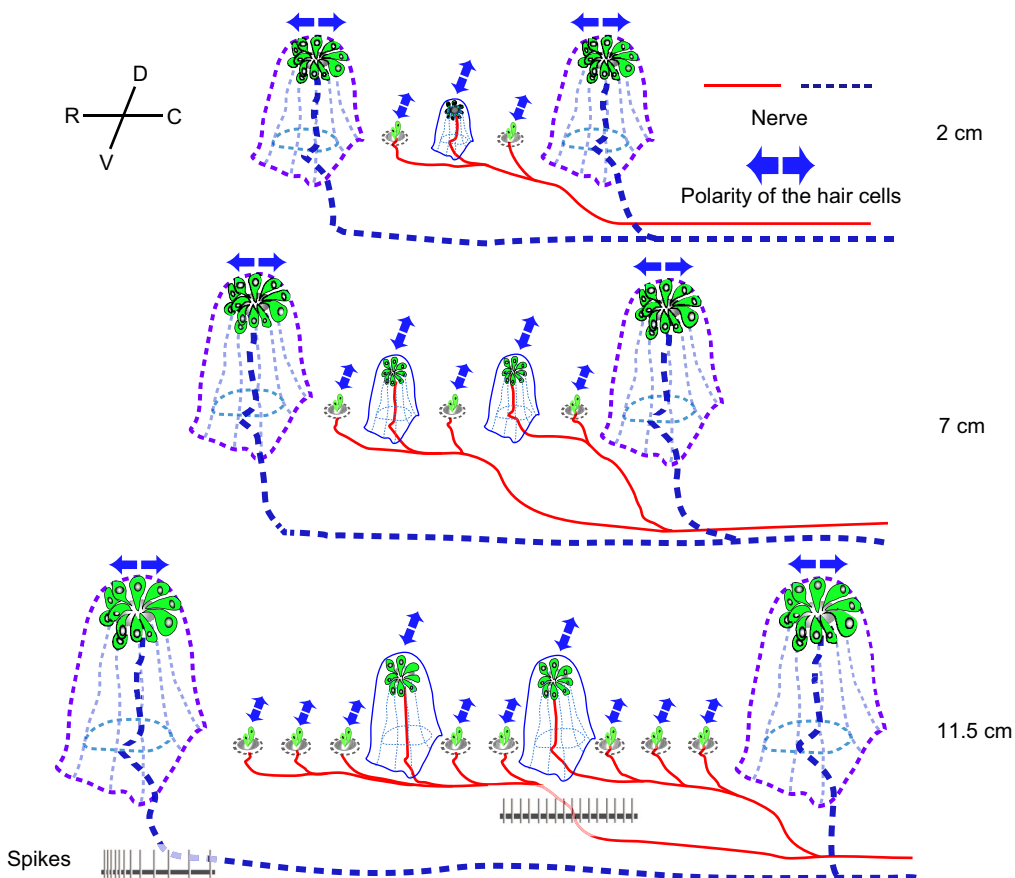


**Fig. 6. Schematic drawing illustrating NM growth patterns in pufferfish.**

Short NMs show an extreme proliferation during fish growth. When fish reached a body length of 11.5 cm, the height of the pedestals for tall and medium NMs reached a stable value. Note that the two NMs are innervated by a separate nerve fiber. In the drawings shown here, the single tall NM is innervated by a separate afferent fiber (in blue), whereas the fiber that innervates the two medium NMs also innervates several neighboring short NMs. Spike activity for the two afferent types is shown for a 11.5 cm pufferfish. Arrows indicate hair cell orientation: C, caudal; D, dorsal; R, rostral; V, ventral.

lower spontaneous firing rate (Liao and Haehnel, 2012). If an afferent fiber innervates only one NM, it has a lower threshold, a greater sensitivity and a higher spontaneous rate (Liao and Haehnel, 2012). In all fish, each single CN can be considered as a functional unit. If several SNs are innervated by the same afferent nerve fiber, these SNs also form a functional unit.

From our results, we suggest the following. Two functional groups of NMs have developed in pufferfish. Tall NMs are sensitive to water acceleration (similar to CNs), while medium and short NMs are sensitive to water velocity (similar to SNs). This unusual lateral line system may provide pufferfish with hydrodynamic information not only under normal conditions but also when the animal is inflated and the lateral line grooves are distorted.

#### Acknowledgements

We deeply appreciate the contributions of Mr Genyu Zhang and Mr Yonghai Shi (Shanghai Fishery Research Institute) for providing the *Takifugu obscurus* embryos and adult fish.

#### Competing interests

The authors declare no competing or financial interests.

#### Author contributions

Conceptualization: J.S., C.L.; Methodology: C.L., X.W., J.W., J.S.; Software: C.L., J.W., X.Z.; Validation: X.W., J.W., C.F., J.S.; Formal analysis: C.L., J.S., X.W., J.W.; Investigation: C.L., X.W., J.W., J.S.; Resources: H.G., J.S.; Data curation: C.L.; Writing - original draft: C.L., J.W., J.S.; Writing - review & editing: J.S., X.W., C.F.; Visualization: C.L., J.S.; Supervision: J.S., X.W., J.W.; Project administration: H.G., J.S.; Funding acquisition: J.S., C.L., X.W.

#### Funding

This project was supported by the funding program for outstanding dissertations of Shanghai Ocean University, Graduate Students Program (to C.L.), Shanghai

University First-Class Disciplines Project of Fisheries, Sensory Neurobiology A2-2019-14-001-4 (to J.S.), National Natural Science Foundation of China (No. 30970365) (to J.S.), and the National Science Foundation for Young Scientists of China (grant number 41306097) (to X.W.).

#### References

- Beckmann, M., Eros, T., Schmitz, A. and Bleckmann, H. (2010). Number and distribution of superficial neuromasts in twelve common European cypriniform fish and their relationship to habitat occurrence. *Internat. Rev. Hydrobiol.* **95**, 273-284.
- Blaxter, J. H. S. (1987). Structure and development of the lateral line. *Biol. Rev.* **62**, 471-514.
- Bleckmann, H. (1994). *Reception of Hydrodynamic Stimuli in Aquatic and Semiaquatic Animals*. New York: G. Fischer Verlag.
- Bleckmann, H. and Zelick, R. (2009). Lateral line system of fish. *J. Integr. Zool.* **4**, 13-25.
- Coombs, S. (2001). Smart skins: information processing by lateral line flow sensors. *Autonomous Robots* **11**, 255-261.
- Dijkgraaf, S. (1963). The functioning and significance of the lateral-line organs. *Biol. Rev.* **38**, 51-105.
- Ghysen, A. and Dambly-Chaudière, C. (2007). The lateral line microcosmos. *Genes Dev.* **21**, 2118-2130.
- Ghysen, A., Wada, H. and Dambly-Chaudière, C. (2014). Patterning the posterior lateral line in teleosts: evolution of development. In *Flow Sensing in Air and Water* (ed. H. Bleckmann, J. Mogdans and S. L. Coombs), pp. 295-318. New York: Springer.
- Holcroft, N. I. and Wiley, E. O. (2008). Acanthuroid relationships revisited: a new nuclear gene-based analysis that incorporates tetraodontiform representatives. *Ichthyol. Res.* **55**, 274.
- Kroese, A. B. and Schellart, N. A. (1992). Velocity- and acceleration-sensitive units in the trunk lateral line of the trout. *J. Neurophysiol.* **68**, 2212-2221.
- Liao, J. C. and Haehnel, M. (2012). Physiology of afferent neurons in larval zebrafish provides a functional framework for lateral line somatotopy. *J. Neurophysiol.* **107**, 2615-2623.
- Marshall, N. J. (1986). Structure and general distribution of free neuromasts in the black goby, *Gobius niger*. *J. Mar. Biol. Assoc. UK* **66**, 323-333.
- Marshall, N. J. (1996). Vision and sensory physiology the lateral line systems of three deep-sea fish. *J. Fish. Biol.* **49**, 239-258.

- Mekdara, P. J., Schwalbe, M. A. B., Coughlin, L. L. and Tytel, E. D.** (2018). The effects of lateral line ablation and regeneration in schooling giant danios. *J. Exp. Biol.* **221**, jeb175166.
- Mogdans, J., Engelmann, J., Hanke, W. and Kröther, S.** (2003). The fish lateral line: how to detect hydrodynamic stimuli. In *Sensors and Sensing in Biology and Engineering* (ed. F. G. Barth, J. A. C. Humphrey and T. W. Secomb), pp. 173-185. Vienna: Springer.
- Mohr, C. and Görner, P.** (1996). Innervation patterns of the lateral line stitches of the clawed frog, *Xenopus laevis*, and their reorganization during metamorphosis. *Brain Behav. Evol.* **48**, 55-69.
- Montgomery, J. C., Baker, C. F. and Carton, A. G.** (1997). The lateral line can mediate rheotaxis in fish. *Nature* **389**, 960-963.
- Münz, H.** (1979). Morphology and innervation of the lateral line system in *Sarotherodon niloticus* (L.) (Cichlidae, Teleostei). *Zoomorphol.* **93**, 73-86.
- Münz, H.** (1985). Single unit activity in the peripheral lateral line system of the cichlid fish *Sarotherodon niloticus* L. *J. Comp. Physiol. A.* **157**, 555-568.
- Nakae, M. and Sasaki, K.** (2005). The lateral line system and its innervation in the boxfish *Ostracion immaculatus* (Tetraodontiformes: Ostraciidae): description and comparisons with other tetraodontiform and perciform conditions. *Ichthyol. Res.* **52**, 343-353.
- Nakae, M. and Sasaki, K.** (2010). Lateral line system and its innervation in Tetraodontiformes with outgroup comparisons: descriptions and phylogenetic implications. *J. Morphol.* **271**, 559-579.
- Song, J. K. and Northcutt, R. G.** (1991a). Morphology, distribution and innervation of the lateral-line receptors of the Florida gar, *Lepisosteus platyrhincus*. *Brain Behav. Evol.* **37**, 24-37.
- Song, J. K. and Northcutt, R. G.** (1991b). The primary projections of the lateral-line nerves of the Florida gar, *Lepisosteus platyrhincus*. *Brain Behav. Evol.* **37**, 38-63.
- Song, L. Z., Song, J. K. and Wang, X. J.** (2010). A postembryonic study on the morphological and growth pattern of the lateral line system in the pufferfish *Takifugu obscurus*. *Chinese J. Zool.* **45**, 19-29.
- Wada, H., Hamaguchi, S. and Sakaizumi, M.** (2008). Development of diverse lateral line patterns on the teleost caudal fin. *Dev. Dyn.* **237**, 2889-2902.
- Wang, X. J., Zhao, S., Li, C., Liu, X. and Song, J. K.** (2015). Neural basis of the stress response in a pufferfish, *Takifugu obscurus*. *J. Integr. Zool.* **10**, 133-140.
- Webb, J. F.** (1989). Gross morphology and evolution of the mechanoreceptive lateral-line system in teleost fishes. *Brain Behav. Evol.* **33**, 34-53.
- Zhao, S., Song, J. K. and Wang, X. J.** (2010). Functional morphology of puffing behavior in pufferfish (*Takifugu obscurus*). *Zool. Res.* **31**, 539-549.